A novel actin–microtubule cross-linking kinesin, NtKCH, functions in cell expansion and division

Jan Klotz and Peter Nick

Molecular Cell Biology, Botanical Institute, and Center for Functional Nanostructures (CFN), Karlsruhe Institute of Technology (KIT), Kaiserstrasse 2, D-76131 Karlsruhe, Germany

Summary

• Kinesins with a calponin homology domain (KCHs) have been identified recently as a plant-specific subgroup of the kinesin-14 family and are suspected to act as microtubule–actin filament cross-linkers. The cellular function, however, has remained elusive.

• In order to address the function of KCHs, we isolated NtKCH, a novel KCH homologue from tobacco BY-2 cells. Following synchronization, NtKCH transcripts were shown to be abundant during mitosis, whereas, during interphase, expression was low.

• Using fluorescent-tagged cell lines and immunolabelling techniques, the localization of tobacco KCH was found to differ depending on the cell cycle. During interphase, NtKCH mainly associated with cortical microtubules, whereas a subfraction also co-localized with perinuclear actin cables. In dividing cells, NtKCH accumulated at the pre-prophase band and at the phragmoplast. However, it remained absent from spindle microtubules, but, instead, concentrated at two agglomerations in proximity to the two cell poles.

• This work develops a detailed model for the dual localization and function of NtKCH during cell division vs cell expansion. This model implies two dynamic states of KCHs that differ with regard to actin interaction. This allows the modulation of force generation by KCH in a cell cycle-dependent capture mechanism.

Introduction

Plant cell growth and division are based on a tight interaction and cross-talk between microtubules and actin microfilaments (for a review, see Wasteneys & Galway, 2003; Collings, 2008). During interphase, both cytoskeleton elements are arranged in close proximity in the cortical layer and microtubules are often cross-linked to filamentous actin, as demonstrated by various microscopic studies (Collings, 2008; Deeks *et al.*, 2010). Cortical microtubules (cMTs) define the axis of cell expansion during cell elongation by guiding cellulose-synthesizing complexes, and hence control the orientation of cellulose microfibrils in the cell wall (Paredez *et al.*, 2006; for a review, see Nick, 2008). However, investigations on actin mutants and treatments with actin-disrupting drugs have demonstrated that actin microfilaments are also required for cell elongation (Collings, 2008; Petrásek & Schwarzerová, 2009), probably associated with cMTs. During mitosis, microtubules and actin filaments co-exist and co-operate in the pre-prophase band (PPB) and the phragmoplast (Traas *et al.*, 1987; Mineyuki, 1999; Sano *et al.*, 2005). Whether and to what extent actin participates in the organization of the spindle is still under debate (Kumagai & Hasezawa, 2001; Yasuda *et al.*, 2005; Panteris, 2008).

In animal and fungal cells, various proteins have been identified that mediate interaction between both cytoskeletal elements (Goode *et al.*, 2000; Rodriguez *et al.*, 2003). However, reports on their plant homologues have remained scarce. Kinesins with a calponin homology domain (KCHs) have been described as a distinct subset of the kinesin-14 family (Tamura *et al.*, 1999; Richardson *et al.*, 2006). As members of this subset have not been identified from animals and fungi, KCHs are assumed to be unique to higher plants (Richardson *et al.*, 2006). KCHs contain an internal kinesin motor flanked by two coiled-coil regions and harbour an additional calponin homology (CH) domain at the N-terminus of the protein (Reddy, 2001; Richardson *et al.*, 2006). The CH domain is known as a typical actin-binding motif that is often found in various actin-associated proteins and in proteins involved in cell signalling (Gimona *et al.*, 2002; Korenbaum & Rivero, 2002).

To date, several KCH members have been reported to bind actin *in vitro* and *in vivo* and have been implicated in cross-linking microtubules and actin filaments (Preuss *et al.*, 2004; Frey *et al.*, 2009; Xu *et al.*, 2009; Buschmann *et al.*, 2011; Umezu *et al.*, 2011). GhKCH1 and GhKCH2 have been shown to co-localize with longitudinal actin cables and transversely oriented microtubules in the cell cortex, and hence are associated with a putative role in the rapid elongation of cotton fibres during interphase (Preuss *et al.*, 2004; Xu *et al.*, 2009). An additional function during mitosis was postulated for GhKCH2, as the kinesin was also present in the phragmoplast midzone of dividing root tip cells. More recently, green fluorescent protein (GFP) fusions of AtKinG from *Arabidopsis thaliana* transiently

expressed in BY-2 cells were found to decorate cMTs in interphase, as well as PPB and phragmoplast during mitosis (Buschmann *et al.*, 2011).

Our group has demonstrated previously the co-localization of microtubules and filamentous actin by OsKCH1 in both cycling and noncycling cells, which therefore seems to be a general feature of KCHs (Frey *et al.*, 2009; Frey, 2010). We further analysed OsKCH1-deficient rice mutants and overexpressing BY-2 cells and obtained opposite cell elongation phenotypes as a result of gene knock-down and overexpression. In addition, we showed that the overexpression of OsKCH1 delayed nuclear positioning at the onset of mitosis in BY-2 cells. A simple working model may be that the primary target of KCHs is cell division, and that the resulting elongation phenotypes are a result of an extended period of cell expansion. Alternatively, KCHs could interfere with the organization of the cortical cytoskeleton filaments and thus fulfil a direct additional function during interphase. In *A. thaliana*, seven copies of KCH genes have been identified (Reddy & Day, 2001), suggesting that various KCH members might convey different functions during the cell cycle. An alternative scenario assumes that a single KCH could interact differentially with various cytoskeletal arrays depending on the respective phase of the cell cycle. This would imply that the biochemical properties of KCHs can be modified, for instance by association with different interaction partners, leading to an alternation between different cell biological functions. However, the cellular and molecular details underlying such a molecular switch are far from understood.

In order to discriminate between these concurrent models, we decided to use tobacco BY-2 cells as a suitable model, as they are fast-growing, large cells that can be synchronized to a high degree (Nagata *et al.*, 1992). To address the function of KCH in the homologous system, we identified and functionally characterized NtKCH, a new KCH member from tobacco. Our results demonstrate the existence of two KCH subpopulations, one motile and associated with microtubules, and the other nonmotile and associated with both microtubules and actin filaments, each acting during different phases of the cell cycle.

Materials and Methods

Isolation of a KCH from *Nicotiana tabacum*

A cDNA library was constructed from BY-2 suspension cells (*Nicotiana tabacum* L., cv Bright Yellow 2) pooled from day 1 to day 7 after subcultivation. For this purpose, aliquots of 100 mg medium-free cells were immediately frozen in liquid nitrogen, ground in a TissueLyser (Qiagen, Hilden, Germany), and total RNA was extracted with an RNeasy plant mini kit following the protocol of the manufacturer (Qiagen), including an on-column digest of genomic DNA with RNase-free DNAse I (Qiagen). The RNA integrity was checked by loading 1 µg RNA on a 1% (w/v) agarose gel; 1 µg RNA from each sample was used as a template for reverse transcription with M-MuLV (NEB, Frankfurt, Germany) and Oligo(dTs) according to the protocol of the manufacturer, and subsequently pooled to a BY-2 cDNA library.

A set of degenerated primers was designed to identify a KCH homologue from *N. tabacum*. For this reason, an alignment of KCH sequences from *Oryza*, *Arabidopsis*, *Gossypium*, *Vitis* and *Populus* was used as a template and primers were set to highly conserved sequence regions. A PCR with Phusion-Polymerase (Finnzymes, Espoo, Finland) and the degenerated primer pair NtKCH_deg-fw (5′-GAGGAAGAATTTAGGCTTGG-3′) and NtKCH_deg-rv (5′-CTTATATGTCTGATTGGGACC-3′) amplified a fragment of 2078 bp, including a CH domain and the conserved kinesin motor. This fragment served as a template in 5′-RACE-PCR and 3′-RACE-PCR (RACE, rapid amplification of cDNA ends) using the GeneRACER-Kit (Invitrogen, Karlsruhe, Germany) to obtain a full-length tobacco-KCH cDNA. The kinesin gene was verified by sequencing (GATC, Konstanz, Germany). Subsequently, the gene-specific primers NtKCH_fl-fw (5′-CCTGTTTAT CCTCTCTGACC-3′) and NtKCH_fl-rv (5′-AGCAGCTTA GTTCACATCC-3′) were designed and applied for end-to-end amplification of the NtKCH coding region. The PCR product was inserted into pCR4-TOPO by a TOPO-TA-cloning reaction (Invitrogen), which was then used as a cDNA clone for further plasmid construction. The nucleotide sequence of NtKCH has been submitted to GenBank (accession number JF835913).

Sequence analysis of NtKCH

Sequence motifs and domains were analysed using SMART (http://smart.embl-heidelberg.de/). Kinesin motor domains of NtKCH, AtKatD, GhKCH2 and DmNCD were aligned using the ClustalW2 tool at EBI (http://www.ebi.ac.uk/Tools/clustalw2/index.html). Coiled-coil domains were predicted according to the Lupas algorithm (Lupas *et al.*, 1991) in COILS (http://www.ch.embnet.org/software/COILS_form.html). To construct a phylogenetic tree, putative members of the KCH subgroup from *A. thaliana*, *Gossypium hirsutum* and *Oryza sativa* were identified in Swiss-Prot∕TrEMBL via a BLAST search using AtKatD (Tamura *et al.*, 1999) as a template. The protein sequences were aligned by the ClustalW2 tool and the alignment was transferred to PhyML3.0 (Guindon & Gascuel, 2003; Guindon *et al.*, 2010) for further phylogenetic analysis using a maximum likelihood approach. The phylogenetic tree was obtained by a heuristic search method with a random stepwise addition of sequences. Bootstrap support values were obtained from 100 replicates. The resulting tree file was visualized with iTOL (Letunic & Bork, 2007) and rooted arbitrarily using AtARK1 from *A. thaliana* (Sakai *et al.*, 2008) as an outgroup. Protein sequence data of the phylogenetic analysis can be accessed in Swiss-Prot∕TrEMBL under the following accession numbers: AtARK1 (Q9SV36), AtKP1 (Q8W1Y3), GhKCH1 (Q5MNW6), GhKCH2 (A4GU96), AtKatD (O81635), OsKCH1 (Q0IMS9), AtKatA (Q07970), Q10MN5, B9FL70, B9EUM5, Q9FHD2, Q9SS42, AtKinG (E1ACC4), O22260, O80491, OsKCBP (Q7XPJ0), AtKCBP (Q9FHN8), AtKatB (P46864), DmNCD (P20480), DmKHC (P17210), ScKar3 (P17119), AtKatC (P46875), XlKHC (A5XAW2), HsKHC (P33176).

Plasmid construction

For stable transformation, a cauliflower mosaic virus (CaMV) 35S promoter-driven N-terminal GFP fusion of NtKCH (GFP-NtKCH) was generated via Gateway technology (Hartley *et al.*, 2000). The full-length coding sequence of NtKCH (1–3003 bp) was amplified from the previously described cDNA clone by PCR using NtKCH_Entry-fw (5′-*GGGGACAAGTTTGTACAAAAA-AGCAGGCT*GCATGGCGGCCTATGGAGCATTGTCTG-3′) as forward primer and NtKCH_Entry-rv (5′-*GGGGACCA-CTTTGTACAAGAAAGCTGGGT*CCTACTTCCTGTTTCCT-GCTTTTCGC-3′) as reverse primer. The PCR product containing the appropriate *att*B-sites (italic) was first recombined into the entry plasmid pDONR/Zeo (Invitrogen) and then cloned into the binary plasmid pK7WGF2 (Karimi *et al.*, 2002). For construction of the red fluorescent protein (RFP)-FABD2 fusion, FABD2 (amino acids 325–687) was transferred from the entry-clone 'pDONR/Zeo-FABD2' (Maisch *et al.*, 2009) into the binary plasmid pH7WGR2 (Dr R. Y. Tsien, University of California, San Diego, CA, USA; Campbell *et al.*, 2002) by a Gateway LR reaction. All construct sequences were verified by sequencing (GATC).

RNA extraction and semi-quantitative reverse transcription-polymerase chain reaction (RT-PCR)

Total RNA from tobacco BY-2 cells was isolated and reverse transcription was performed as described above. For amplification of the cDNA, a PCR was carried out in 25 µl using standard Taq polymerase (NEB) with the following cycling parameters: 5 min at 94°C, 25 × (1 min at 94°C, 30 s at 56°C, 45 s at 72°C), 5 min at 94°C. The number of PCR cycles was chosen such that the amplification of templates for all primers was still in an exponential range and the PCR products were clearly visible on agarose gels. The primer pair NtKCH_squant-fw (5′-CTGCAGATGTCAAA-GAGC-3′) and NtKCH_squant-rv (5′-CTTTGTCTACCC-ACTCACC-3′) was designed to amplify a diagnostic 363-bp amplicon that was specific for NtKCH. All results were normalized using the constitutively expressed glyceraldehyde-3-phosphate dehydrogenase (GAPD) gene as an internal standard, which was amplified with the primers GAPD-fw and GAPD-rv (Hu *et al.*, 2010). PCR products were separated on 2% (w/v) agarose gels, stained with SYBR Safe (Invitrogen) and recorded by digital imaging (Rainbow camera system; Hama, Monheim, Germany). Grey values of NtKCH amplicons were quantified by analysis in ImageJ (Release 1.42q; http://rsbweb.nih.gov/ij/; National Institutes of Health, Bethesda, MD, USA) and normalized to the GAPD signal. Mean values and standard errors (SEs) were calculated from at least three independent experiments.

Cell culture

Tobacco BY-2 cells were maintained in liquid Murashige and Skoog (MS) medium and subcultured weekly (Nagata *et al.*, 1992). The cells were shaken in darkness at 25°C and 150 rpm on an orbital shaker IKA KS260 (IKA Labortechnik, Staufen, Germany). Stably transformed BY-2 cultures of GFP-NtKCH and GFP-NtKCH/RFP-FABD2 were maintained in liquid MS medium supplemented with 100 mg l^{-1} kanamycin or 100 mg l^{-1} kanamycin plus 50 mg l^{-1} hygromycin in the case of co-transformation.

Cell cycle synchronization of BY-2 cells

For cell cycle synchronization, a two-step protocol was applied as described by Samuels *et al.* (1998) with some modifications. Stationary, 7-d-old cells were subcultured in MS medium containing 4 mM hydroxyurea (HU; Sigma, Taufkirchen, Germany). After 24 h, HU was washed out by three successive washing steps with fresh medium. The cells were resuspended in fresh MS medium and returned to the orbital shaker for a further 3 h, when propyzamide (Sigma) was added to a final concentration of 6 µM. Cell cycle progression was monitored by measuring the mitotic index (MI) at appropriate time intervals. At a mitotic peak of 60%, cells were released from propyzamide inhibition by three further washing steps in medium free of propyzamide, and transferred into fresh MS medium.

Determination of MI

Cell cycle progression was monitored by measuring MI, defined as the relative frequency of dividing cells. For this purpose, cells were fixed in Carnoy fixative (3 : 1 100% ethanol : glacial acetic acid, plus 0.25% Triton X-100) and nuclei were stained using Hoechst 33 258 substance (Sigma) at a final concentration of 1 µg ml^{-1}. Nuclear morphology was immediately investigated under a fluorescence microscope. For each time point, at least 500 cells were counted in three replicates, and mean values and SEs were calculated.

Stable transformation of BY-2 cells

BY-2 cells were either transformed with GFP-NtKCH or co-transformed with GFP-NtKCH and RFP-FABD2 using *Agrobacterium tumefaciens* (strain LBA4404) according to the 'TAMBY2' method, which has been described in detail by Buschmann *et al.* (2011). In order to adapt to stable transformation, we included an additional selection step. Co-cultivated cell suspension droplets, grown on solid Paul's medium, were transferred on selective plates after 3 d. The selective plates were composed of MS medium with 0.8% Danish Agar-Agar (Roth, Karlsruhe, Germany), 100 mg l^{-1} cefotaxime sodium and either 100 mg l^{-1} kanamycin (GFP-NtKCH) or a combination of 100 mg l^{-1} kanamycin and 50 mg l^{-1} hygromycin (GFP-NtKCH/RFP-FABD2). The plates were incubated at 25°C in the dark, and calli were raised from transformed cells. Suspension cultures were established from these calli and maintained in liquid MS medium supplemented with the appropriate antibiotics.

Immunostaining of microtubules

Microtubules of tobacco BY-2 cells were visualized by indirect immunofluorescence as described previously in Frey *et al.* (2010)

using the primary antibodies DM1A and ATT from mouse (Breitling & Little, 1986), and a secondary TRITC-conjugated antibody against mouse IgG (Sigma).

Treatments with latrunculin B and oryzalin

Oryzalin (10 µM) or latrunculin B (10 µM) (both from Sigma) was added at day 1 after subculture to BY-2 cells stably co-expressing GFP-NtKCH/RFP-FABD2, and the cells were incubated for a further 1 h under standard cultivation conditions. As a control, the co-expressing cells were treated in the same way with the solvent dimethylsulfoxide (DMSO).

Microscopy and image analysis

Cells were examined under an AxioImager Z.1 microscope (Zeiss, Jena, Germany) equipped with an ApoTome microscope slider for optical sectioning and a cooled digital CCD camera (AxioCam MRm). For localization studies, cells were viewed using a ×63 plan apochromate oil-immersion objective. RFP/TRITC and GFP fluorescences were observed through the filter sets 43 HE (excitation at 550 nm, beam splitter at 570 nm and emission at 605 nm) and 38 HE (excitation at 470 nm, beam splitter at 495 nm and emission at 525 nm), respectively. For the determination of MI, nuclear morphology was determined by a ×20 objective using the filter set 49 DAPI (excitation at 365 nm, beam splitter at 395 nm and emission at 445 nm) to visualize Hoechst 33 258 staining. Objectives and filter sets were purchased from Zeiss. Image analyses were performed using AxioVision (Release 4.8; Zeiss) and ImageJ software.

Results

Isolation and sequence analysis of NtKCH

A new KCH could be identified from *N. tabacum* by screening a BY-2 cDNA library. We isolated a fragment of *c.* 2 kb, including a CH domain and a highly conserved kinesin motor domain, by RT-PCR techniques with degenerated primers. A nucleotide BLAST search in GenBank with the obtained fragment sequence yielded high similarity (96%) with a 471-bp mRNA encoding a fragment of a kinesin-like polypeptide from *N. tabacum* (TBK9, GenBank accession number AB053096.1; Matsui *et al.*, 2001). In addition, a similarity of 79% to the well-characterized GhKCH2 from *G. hirsutum* (Xu *et al.*, 2007, 2009) was found. We therefore assumed that the isolated fragment might correspond to the prolonged TBK9 sequence, and represents a new KCH from tobacco. After 5'-RACE and 3'-RACE, we obtained the full-length coding region. The nucleotide sequence encodes for a predicted protein of 1001 amino acids, which we named NtKCH (for *N. tabacum* *k*inesin with *c*alponin *h*omology domain), and has a calculated molecular mass of 110 kDa.

SMART analysis revealed a CH domain at the N-terminus (amino acids 39–157) and a highly conserved motor domain in a central position (amino acids 387–721), including an ATP-binding consensus and a putative microtubule binding site (Yang *et al.*, 1989) (Fig. 1b). An alignment of the NtKCH motor core (Fig. 1a) showed 85% amino acid identity to the corresponding region (amino acids 400–734) of GhKCH2 (Xu *et al.*, 2007), and 75% identity to the motor core (amino acids 395–730) of AtKatD from *Arabidopsis* (Tamura *et al.*, 1999). Furthermore, we detected the 14-amino-acid neck-linker region which conforms to the consensus neck motif characteristic for minus-end-directed kinesins, such as DmNCD from fruit fly (Fig. 1a, marked with asterisks) (Endow, 1999). Secondary structure prediction in COILS suggested two short regions which are likely to form coiled-coils upstream and at the very C-terminal end of the kinesin motor domain (Fig. 1b). Such α-helical structures with characteristic periodic heptapeptide repeats are often associated with protein dimerization or oligomerization (Lupas *et al.*, 1991).

To determine the evolutionary relationship between NtKCH and other kinesins, especially kinesin-14s, a phylogenetic tree was constructed at amino acid level. The tree in Fig. 1(c) shows that NtKCH clusters into the kinesin-14 subgroup of CH domain-containing kinesins with a close relationship to GhKCH2 from cotton and AtO22260 (AGI number: At2g47500), an uncharacterized kinesin-related protein from *A. thaliana*. KCHs from higher plants cluster into four different clades, each containing at least one KCH member from all tested species (Frey *et al.*, 2010). NtKCH is classified into the most expanded clade together with OsKCH1, AtKatD, GhKCH1 and GhKCH2 (not shown). However, within this clade, the tobacco KCH forms a separate phylogenetic branch, together with GhKCH2 and AtO22260, suggesting conserved functions among these proteins.

Localization pattern of NtKCH in interphase BY-2 cells

The localization pattern of tobacco KCH in the homologous system during the cell cycle should allow some insight into its function. Therefore, a BY-2 suspension cell line was generated, stably expressing a GFP-NtKCH fluorescent fusion construct under the control of a 35S promoter. In interphase cells, a punctate NtKCH signal aligned as transverse thin filaments in the cell cortex (Fig. 2a–c). In addition, strong fluorescence signals were found around the nucleus and along radial filaments which emanate at the nucleus and spread towards the cell periphery (Fig. 2d–f). Identical localization patterns were observed in BY-2 cells transiently transformed with N- and C-terminal fusions of GFP with NtKCH via particle bombardments (not shown). To determine the association between cytoskeleton elements and tobacco KCH, microtubules of the GFP-NtKCH cell line were stained by indirect immunofluorescence. NtKCH clearly decorated TRITC-labelled microtubules of the cortical array in a punctate fashion (Fig. 2j–l; arrows in 2l). However, no GFP fluorescence co-localizing with cMTs could be detected in either a cell line stably expressing free GFP (Fig. 2m–o) or in nontransformed BY-2 cells (not shown), which were stained by the same immunofluorescence technique in control experiments.

To test whether NtKCH also co-localizes with cortical actin filaments, a second tobacco cell line stably co-expressing the

(a)

(b)

(c)
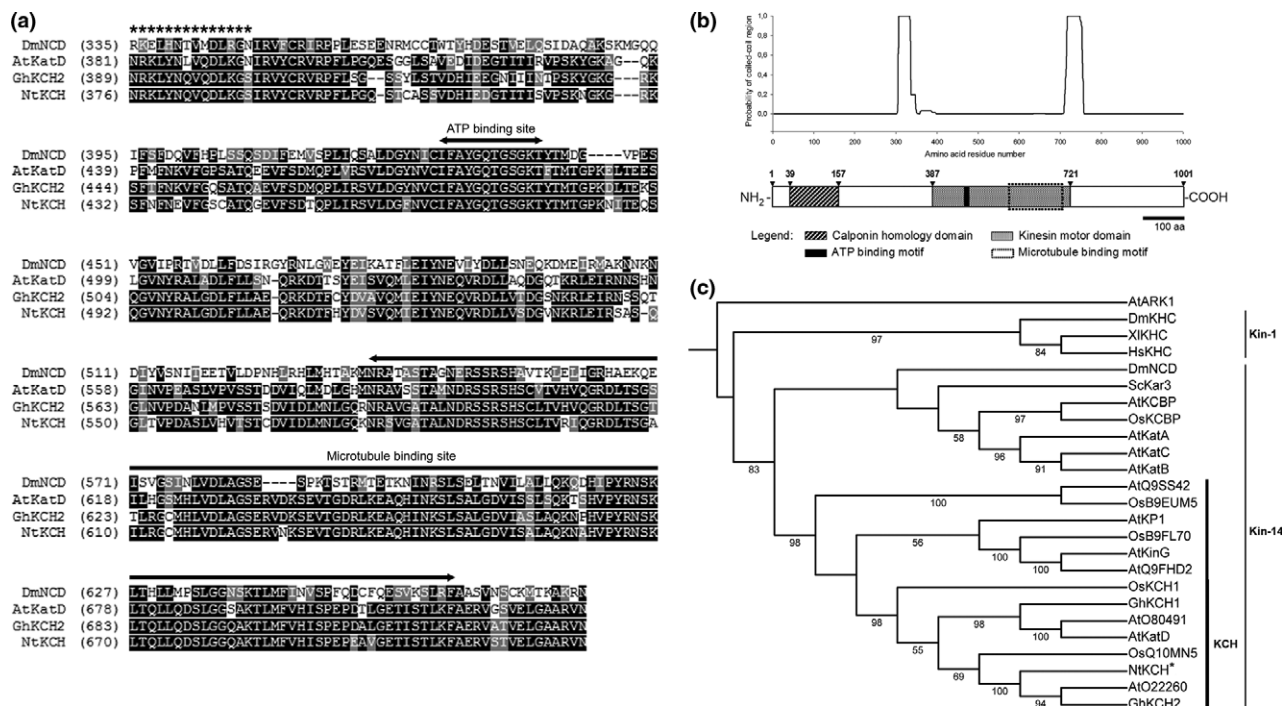
Fig. 1 Sequence analysis of NtKCH from *Nicotiana tabacum*. (a) Alignment of the putative motor core of NtKCH with those of DmNCD and the KCH members AtKatD and GhKCH2. Identical amino acid residues are shaded in black and similar residues are shaded in grey. The ATP-binding consensus and the putative microtubule-binding module are highlighted by thick lines above the sequences. The neck motif of NtKCH is marked with asterisks and matches with the 14-amino-acid stretch associated with minus-end directionality in the kinesin-14 family (Endow, 1999). (b) Coiled-coil prediction and schematic diagram for domain organization in NtKCH. A probability value > 0.5 indicates that the corresponding region probably forms a coiled-coil. Domain analysis by SMART predicts a putative kinesin motor domain in the central region including conserved ATP- and microtubule-binding sites and an N-terminal calponin homology (CH) domain. (c) Phylogenetic relationship of NtKCH (marked by an asterisk) and other members of the KCH subgroup with several plant and animal kinesin-14 proteins and representatives of the kinesin-1 family. The tree was generated by a maximum likelihood approach with a random stepwise addition of protein sequences and routed arbitrarily using AtARK1 as outgroup. Bootstrap support values were obtained from 100 replicates and only values > 50 are shown in the tree. At, *Arabidopsis thaliana*; Dm, *Drosophila melanogaster*; Gh, *Gossypium hirsutum*; Hs, *Homo sapiens*; Nt, *Nicotiana tabacum*; Os, *Oryza sativa*; Sc, *Saccharomyces cerevisiae*; Xl, *Xenopus laevis*. All protein sequence data were obtained from Swiss-Prot/TrEMBL.

GFP-NtKCH construct and an N-terminal RFP fusion of the actin marker FABD2 was established that allowed us to simultaneously visualize the kinesin and actin filaments in living cells. When investigating cortical sections of the co-expressing cell line, we only detected NtKCH signals along transversely oriented microtubules (Fig. 2g), but not on cortical actin filaments which are arranged below the microtubule array (Fig. 2h,i). However, in the midplane cell sections, NtKCH was frequently associated with actin of the perinuclear network and with filaments bridging the nucleus with the cell periphery (Fig. 2d–f; arrows in 2f). Some of the GFP signals were also found along filamentous structures in this region which were not labelled by RFP-FABD2, suggesting that a subfraction of KCH also associates with the intracellular microtubules.

In order to determine whether NtKCH is dynamic, time-lapse studies were conducted. This allowed the observation of an active movement of fluorescent dots along cMTs with an average velocity of 3.26 ± 0.09 µm min^{-1} (Fig. 3a–d; Supporting Information Movie S1). NtKCH associated with the nuclear envelope, however, seemed to be static (Fig. 3e). To test whether the localization of NtKCH was dependent on the integrity of the two cytoskeletal filaments, stably co-transformed GFP-NtKCH/RFP-

FABD2 cells were treated with either latrunculin B or oryzalin. In cells incubated for 1 h with 10 µM oryzalin, cortical NtKCH expression disappeared completely (Fig. S1c), whereas strong KCH signals around the nucleus resisted the microtubule polymerization inhibitor (Fig. S1d, arrowheads). By contrast, treatment of the cells with 10 µM latrunculin B caused the fine cortical actin meshwork to disintegrate, whereas NtKCH expression along transverse cortical filaments remained unaffected (Fig. S1e). The perinuclear NtKCH fluorescence, however, became diffuse and cytoplasmatic, concomitant with the disruption of intracellular actin filaments (Fig. S1f). In control cells incubated with the solvent DMSO under the same conditions, cortical and intracellular NtKCH signals were clearly preserved in filaments (Fig. S1a,b).

During mitosis NtKCH localizes to the PPB and phragmoplast, but not to the spindle

The established transgenic BY-2 cell lines were used as tools to study the cell cycle-dependent localization pattern of tobacco KCH during mitosis. Although the GFP-NtKCH/RFP-FABD2 co-expressors provided information on KCH localization with
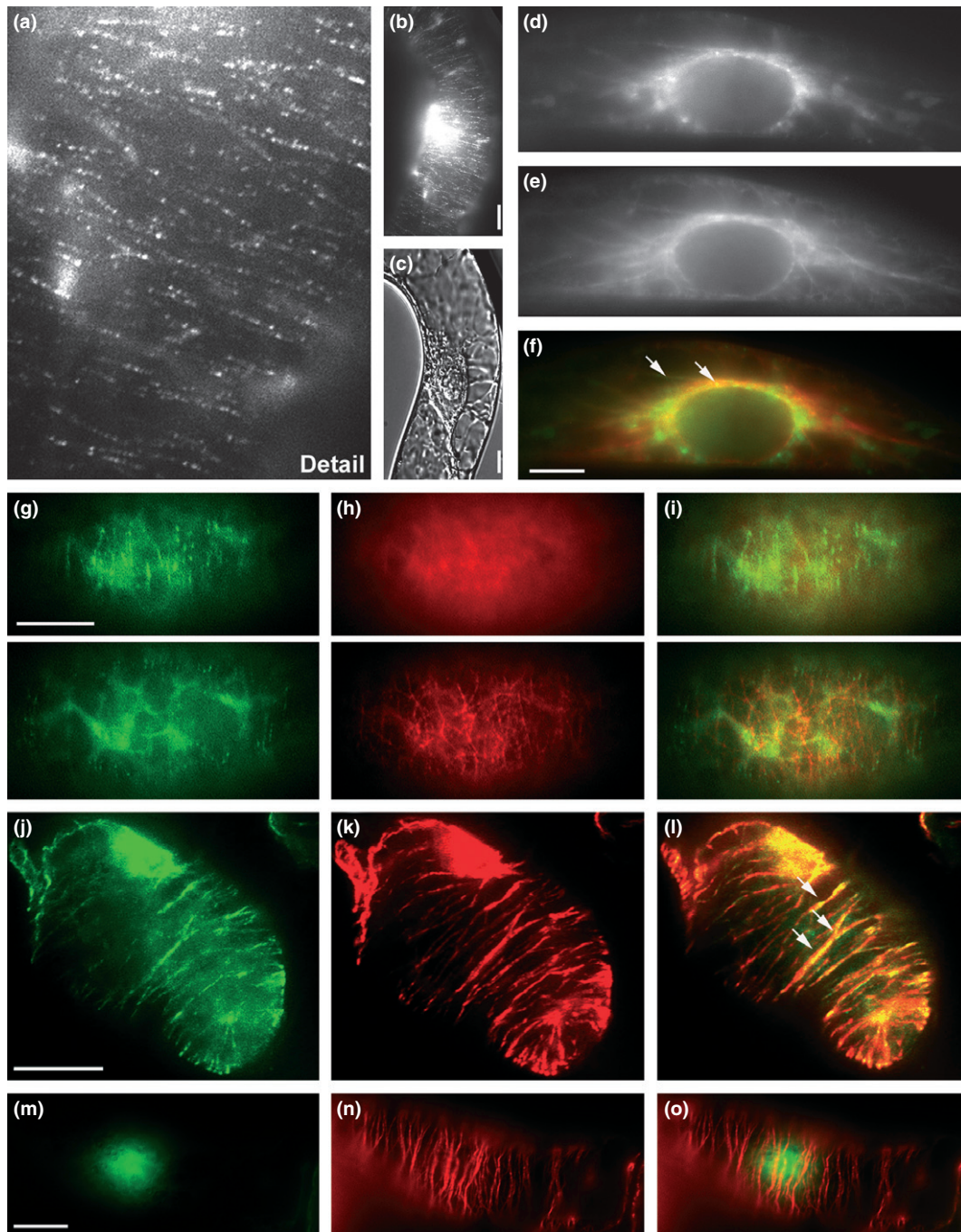
Fig. 2 Localization of GFP-NtKCH in tobacco (*Nicotiana tabacum*) BY-2 cells during interphase. (a–c) A detailed view of the cortical layer of a stably transformed GFP-NtKCH BY-2 cell (a) shows that punctate NtKCH decorates transverse cortical microtubules (cMTs). The corresponding differential inter-ference contrast (DIC) image is given in (c). (d–f) Midplane section of a BY-2 cell co-expressing GFP-NtKCH (d) and the actin marker RFP-FABD2 (e). Arrows highlight NtKCH signals associated with actin filaments of the perinuclear network and with radial actin filaments (note yellow dots in f). (g–i) Cortical sections of the GFP-NtKCH/RFP-FABD2 co-expressors reveal that the KCH (g) does not coincide with cortical actin filaments (h, merged i). (j–l) An immunofluorescence staining of microtubules on fixed GFP-NtKCH cells confirms NtKCH expression along cMTs (arrows in l). (m–o) In a control experi-ment, the microtubules of a BY-2 cell line expressing free GFP were stained by antibodies. Only a diffuse GFP signal around the nucleus can be detected (m) which does not co-localize with the stained microtubules (o). Bars, 10 μm.

respect to actin (Fig. 4a–i), immunostainings of microtubules on fixed GFP-NtKCH cells revealed the putative association of the kinesin with microtubule structures during different phases of cell division (Fig. 4j–u). As controls, microtubules were visual-ized by immunostaining in cells expressing free GFP or in nontransformed cells. Both showed no specific co-localization of signals with microtubules (not shown).

At the onset of plant mitosis, punctate GFP-NtKCH accumu-lated at cMTs of the PPB (Fig. 4a–c). By immunofluorescence staining on fixed GFP-NtKCH cells, the co-localization with

microtubules of the PPB was confirmed (Fig. 4j–l). Additional GFP signals were observed along filament-like structures bridging the nucleus with the PPB during pre-prophase. When cells entered prophase, cortical NtKCH expression declined with the breakdown of the PPB, whereas intracellular GFP signals seemed to accumulate near the prospective spindle poles (Fig. 4o, arrows). During meta- and anaphase, all investigated cells showed a very diffuse GFP signal at the site of chromosome segregation, suggesting that there is no specific association of the kinesin within the spindle. However, a strong accumulation of the tagged protein was observed distal to the spindle poles (Fig. 4d–f, p–r). At the end of telophase, NtKCH expression coincided with the phragmoplast and persisted during all stages of phragmoplast development (Fig. S2; Movie S4). As displayed by immunolocalization (Fig. 4s–u) and treatment with latrunculin B (Fig. S1g), NtKCH clearly associated with the microtubules within the phragmoplast, but remained excluded from the midzone, where short actin filaments accumulated (Fig. 4g–i). However, the bright fluorescence distal to the former spindle poles persisted during this stage. At the end of cytokinesis, when the cell plate had expanded centrifugally and started to fuse with the membrane of the daughter cells, NtKCH expression on the decomposing phragmoplast started to become diffuse again and redistributed to the side of the daughter nuclei facing the new cell wall. As soon as the separation of the cells had been completed and the daughter nuclei had reached their final central position, the diffuse GFP signal was converted into bright fluorescence dots, and was associated with the new nuclear envelopes (Fig. S3).

In order to determine whether the NtKCH associated with phragmoplast microtubules was also dynamic, kymograph analysis was carried out, which revealed that phragmoplast KCH moved with the same average velocity as the KCHs on cMTs during interphase. The movement of the fluorescently labelled dots was directed away from the division site towards the daughter nuclei (Fig. 3j,k; Movie S3).

NtKCH transcripts are upregulated during mitosis in synchronized BY-2 cells

Quantification of NtKCH expression in different tissues of tobacco plants showed variations in gene expression at the level of mRNA. Elevated NtKCH transcription could be observed in

tissue with meristematic activity (not shown). Furthermore, localization studies revealed an association of fluorescently labelled NtKCH with microtubules of the PPB and the phragmoplast in dividing suspension cells. We therefore decided to analyse the RNA profile of NtKCH during cell division by semi-quantitative RT-PCR. For this purpose, tobacco suspension cells were synchronized by sequential treatment with the ribonucleotide reductase inhibitor HU and propyzamide, which prevents polymerization of spindle microtubules. Using this approach, we achieved a high degree of synchronization up to mitotic indices of 65–70%. Cells were collected at the indicated time points during the synchronization procedure. The averaged MI and the averaged relative NtKCH expression from three independent experiments were related to the expression level measured after treating the cell suspension with HU for 24 h. No mitotic events (MI = 0%) could be observed at this time point (Fig. 5a), monitoring the effective S-phase block. At the time of propyzamide removal, c. 60% of the cells were arrested in pro-metaphase; 1–2 h later, MI reached a peak of 65–70%, followed by a successive decline until, 4 h after propyzamide release, nearly all cells had entered interphase again. The abundance of NtKCH transcripts correlated with the mitotic activity of synchronized cells. A strong accumulation of NtKCH transcripts could be observed at the onset of mitosis compared with the expression during the S-phase block. After release from propyzamide, the transcript level successively declined and, 4 h after propyzamide removal, when c. 93% of the cells had re-entered interphase, the mRNA expression was at the same level as during the S-phase block. Low levels of NtKCH transcripts could also be detected when there were no mitotic events (Fig. 5b).

Discussion

Dynamic tobacco KCH moves along cMTs uncoupled from actin

In this study, we isolated a new kinesin with CH from BY-2, NtKCH. We followed its expression and localization through the cell cycle, leading to a model suggesting that NtKCH functions during interphase and cell division (Fig. 6). During interphase, NtKCH decorates cMTs (Fig. 6e–g). The specificity of the co-localization in fixed immunostained cells was confirmed by

Fig. 3 Time-lapse studies on the dynamic behaviour of different NtKCH subpopulations in stable transformed GFP-NtKCH BY-2 cells. (a) Velocity distribution of GFP-NtKCH moving on cortical microtubules (cMTs). The average velocity was 3.26 ± 0.09 µm min^{-1} ($x \pm$ SE; $n = 60$). (b) Comparison of the velocity of NtKCH with minus-end-directed kinesin-14s from plant and animal species and the conventional KHC from fruit fly. (c) Example of an interphase BY-2 cell with a strong expression of GFP-NtKCH on cMTs. The kymograph shown in the bottom right corner represents the dynamic behaviour of the KCH signal marked by a blue arrowhead. The grey bar indicates the time, and the black bar the distance. (d) A representative time-lapse series demonstrating in detail the dynamic behaviour of two of the cortical fluorescence dots (highlighted by red and blue arrowheads). (e) A midplane section through a GFP-NtKCH-expressing cell. Bright dot-like fluorescence speckles accumulate around the nucleus. The representative kymograph illustrates the static behaviour of the perinuclear NtKCH (marked by red arrowheads). (f–i) Inward directed movement of GFP-NtKCH along radial filaments. (g) Detailed view of the NtKCH signal used for the time-lapse series (i) and the corresponding kymograph (h). (i) Time-lapse images of NtKCH on radial filaments. The white arrow in the first image points towards the position of the nucleus. (j, k) NtKCH on phragmoplast microtubules moves away from the division site. The red arrowhead in (j) highlights the GFP signal used for kymograph analysis and the time-lapse image series. (k) For better visualization, the images were inverted. The tilted black bar given in the first image marks the cell plate (CP). The red arrowhead indicates the starting position, and the blue arrowhead the movement away from the cell plate. Dynamic NtKCH on radial filaments and phragmoplast microtubules moves with the same velocity as NtKCH on cMTs. Bars, 10 µm.

(a) $v_{mean} = 3.26 \pm 0.09$ µm min^{-1}
$n = 60$

(b)
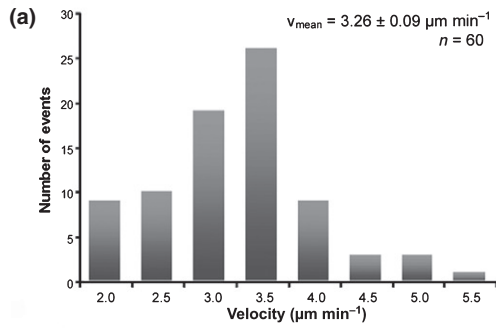
Kinesin	Velocity	Species	Source
NtKCH	3.2 µm min^{-1}	N. tabacum	this work
AtKCBP	10 µm min^{-1}	A. thaliana	Song et al., 1997
AtKatA	9.6 µm min^{-1}	A. thaliana	Marcus et al., 2002
ATK5	6 µm min^{-1}	A. thaliana	Ambrose et al., 2005
ScKar3	1–2 µm min^{-1}	S. cerevisiae	Endow et al., 1994
DmNCD	8–10 µm min^{-1}	D. melanogaster	Chandra et al., 1993
DmKHC	46 µm min^{-1}	D. melanogaster	Hancock & Howard, 1998
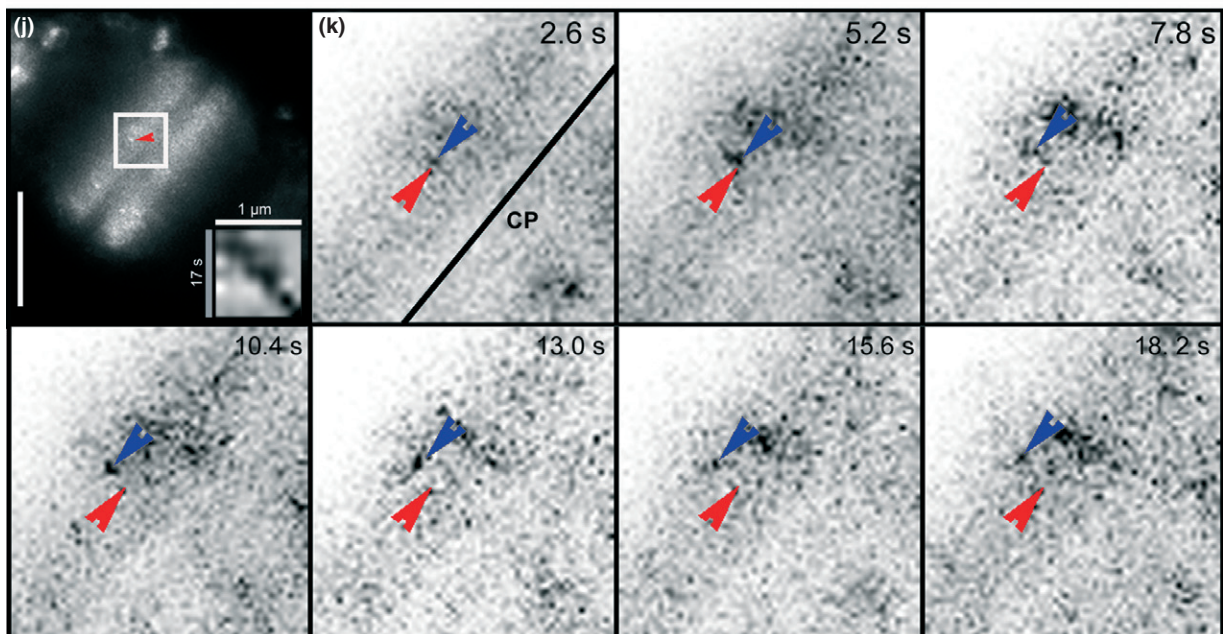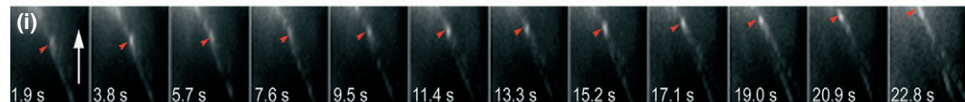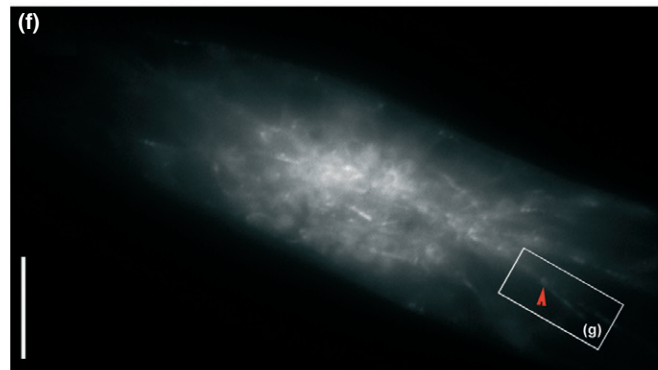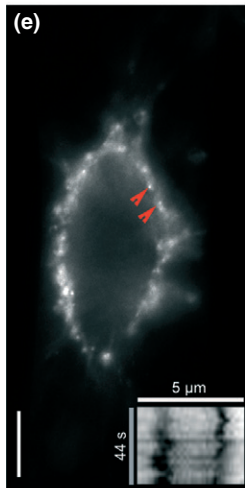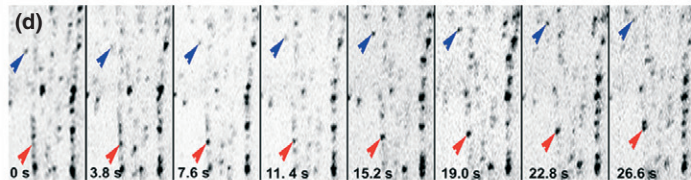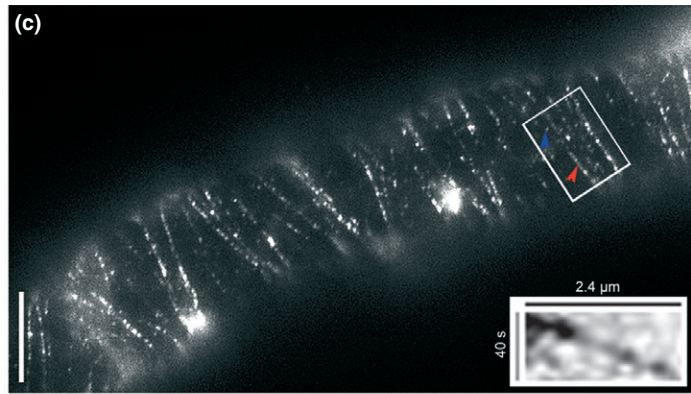
Fig. 4 Expression pattern of NtKCH in tobacco (*Nicotiana tabacum*) BY-2 cells during cell division. (a–i) Localization studies on tobacco BY-2 cells stably transformed with GFP-NtKCH (b, d, g) and the fluorescent actin marker RFP-FABD2 (c, e, h). Merged pictures of both channels are given in (a, f, i). (a–c) In a cortical section of a co-expressing BY-2 cell, the pre-prophase band (PPB) is labelled by dot-like GFP-NtKCH signals (a, b). (d–f) During metaphase, GFP-NtKCH fluorescence is restricted to the poles of the division spindle. (d) Only a diffuse fluorescent signal is visible at the site of chromosome segregation. (g–i) A cell in telophase shows the localization of punctate GFP-NtKCH to microtubule structures of the phragmoplast. The NtKCH signal is absent from the midzone and does not associate with actin filaments of the phragmoplast (i). (j–u) Immunostaining of microtubules (k, n, q, t) in BY-2 cells stably transformed with GFP-NtKCH (j, m, p, s). The merged pictures (l, o, r, u) confirm the localization of NtKCH with mitotic microtubule structures. A cortical section of a pre-prophase cell (j–l) and a z-stack projection of a cell during nuclear envelope breakdown (m–o) demonstrate association with the PPB and the prospective spindle poles (o, highlighted with arrows). (p–r) NtKCH does not co-localize with kinetochore microtubules and is confined to the spindle poles during metaphase. (s–u) At late telophase, NtKCH expression is redistributed and clearly present among phragmoplast microtubules (u). Bars, 10 μm.

controls for background fluorescence or unfused GFP. Furthermore, cortical GFP-NtKCH expression could be disrupted by oryzalin. The binding to cMTs is consistent with published results, where the localization pattern has been analysed by the overexpression of fluorescently tagged proteins (Frey *et al.*, 2009; Buschmann *et al.*, 2011) or by immunostaining (Preuss *et al.*, 2004; Xu *et al.*, 2009). KCHs from cotton are also supposed to interact with cortical actin filaments, most probably via their N-terminal CH domain, and to cross-link MTs and actin, as shown in cotton fibres and *in vitro* studies (Preuss *et al.*, 2004; Xu *et al.*, 2009). Moreover, the rice OsKCH1 localizes to longitudinal actin cables preferentially at the putative cross-points with transverse oriented microtubules (Frey *et al.*, 2009). However, the GFP-NtKCH signal was clearly distinct from the FABD2-labelled cortical actin filaments and was not affected by the actin polymerization inhibitor latrunculin B. This indicates that the NtKCH interacting with cMTs is not coupled to actin. A function of plant kinesins for cell expansion is postulated to be linked to the organization of cMT arrays and/or the microtubule-based movement of cellulose synthases (Cai & Cresti, 2010). We have shown previously that insertion of *Tos17* in the OsKCH1 locus impairs cell elongation in rice coleoptiles, whereas overexpression of OsKCH1 increases cell length in BY-2 cells (Frey *et al.*, 2010). Thus, we believe that mobile cortical NtKCH contributes to cell elongation, possibly by stabilizing transverse arrays of microtubules during interphase.

However, GFP-NtKCH was also observed in PPB and the phragmoplast, where it localized with microtubules as suggested by immunostainings of fixed cells. We verified the specificity and autofluorescence using different control cell lines. The comparison of the localization of fluorescently labelled and immunostained kinesin, together with the observed upregulation of mRNA transcription, suggests that NtKCH is primarily needed during cell division. It is noteworthy that NtKCH on cMTs, PPB and the phragmoplast is dynamic, similar to AtKinG in BY-2 cells which move along cMTs and accumulate at their minus-ends (Buschmann *et al.*, 2011). As for other kinesin-14s, the velocity of NtKCH movement is relatively slow when compared with other kinesin families (Fig. 3b). We observed GFP-NtKCH signals on phragmoplasts moving from the division site towards the daughter nuclei. As microtubules of the phragmoplast are all arranged with their growing plus-end towards the division plane (Euteneuer *et al.*, 1982), we conclude that NtKCH is minus-end-directed, consistent with respective signatures (Endow, 1999) identified *in silico* in the neck-linker region of NtKCH.

Actin-coupled NtKCH around the nucleus is static

We used an advanced *Agrobacterium*-mediated transformation technique to establish a double-transformed BY-2 cell line, expressing a fluorescent NtKCH fusion and the RFP-coupled actin marker FABD2. With this transgenic cell line, we were able, for the first time, to follow simultaneously the localization of KCH with respect to filamentous actin through the entire cell cycle *in vivo*.

In interphase cells, NtKCH accumulated around the nucleus, where it appeared as bright fluorescent speckles clearly different from the punctate signals on cMTs (Fig. 6e,g,h). Time-lapse series showed that the perinuclear speckles were more or less static and often coincided with actin filaments, and with radial actin cables. Furthermore, perinuclear localization was sensitive to latrunculin B. Although these speckles persisted through the whole cell cycle, co-localization with actin was only observed during interphase. The exclusive co-localization of KCHs with perinuclear actin filaments has been reported previously (Frey *et al.*, 2010; Buschmann *et al.*, 2011), and implies that KCHs can differentiate between distinct actin arrays. As actin binding is a common feature of KCHs, which has been demonstrated *in vitro* and *in vivo*, we also conclude that NtKCH may interact with actin directly, consistent with our localization data. However, to test whether co-localization is caused by direct molecular interaction, bimodal fluorescence complementation or Förster resonance studies will be necessary. A part of the GFP-NtKCH signal was also found on filamentous structures not labelled by RFP-FABD2, suggesting that KCH is also associated with perinuclear microtubules and could therefore act as a cross-linker between both cytoskeleton elements.

Therefore, NtKCH seems to be organized into two different subpopulations that co-exist in distinct subcellular regions and differ with respect to their dynamics. The dynamic KCH exclusively binds microtubules and translocates towards their minus-ends. By contrast, static KCH accumulates around the nucleus where it can interact with actin.

NtKCH is dynamically repartitioned during mitosis

Using highly synchronized BY-2 cells, we observed that NtKCH transcripts accumulated at mitosis, indicating cell cycle-dependent transcriptional activation. In a synchronized cell culture of *A. thaliana*, 23 kinesin-like proteins were upregulated during mitosis. Seven of these belonged to the kinesin-14 family,
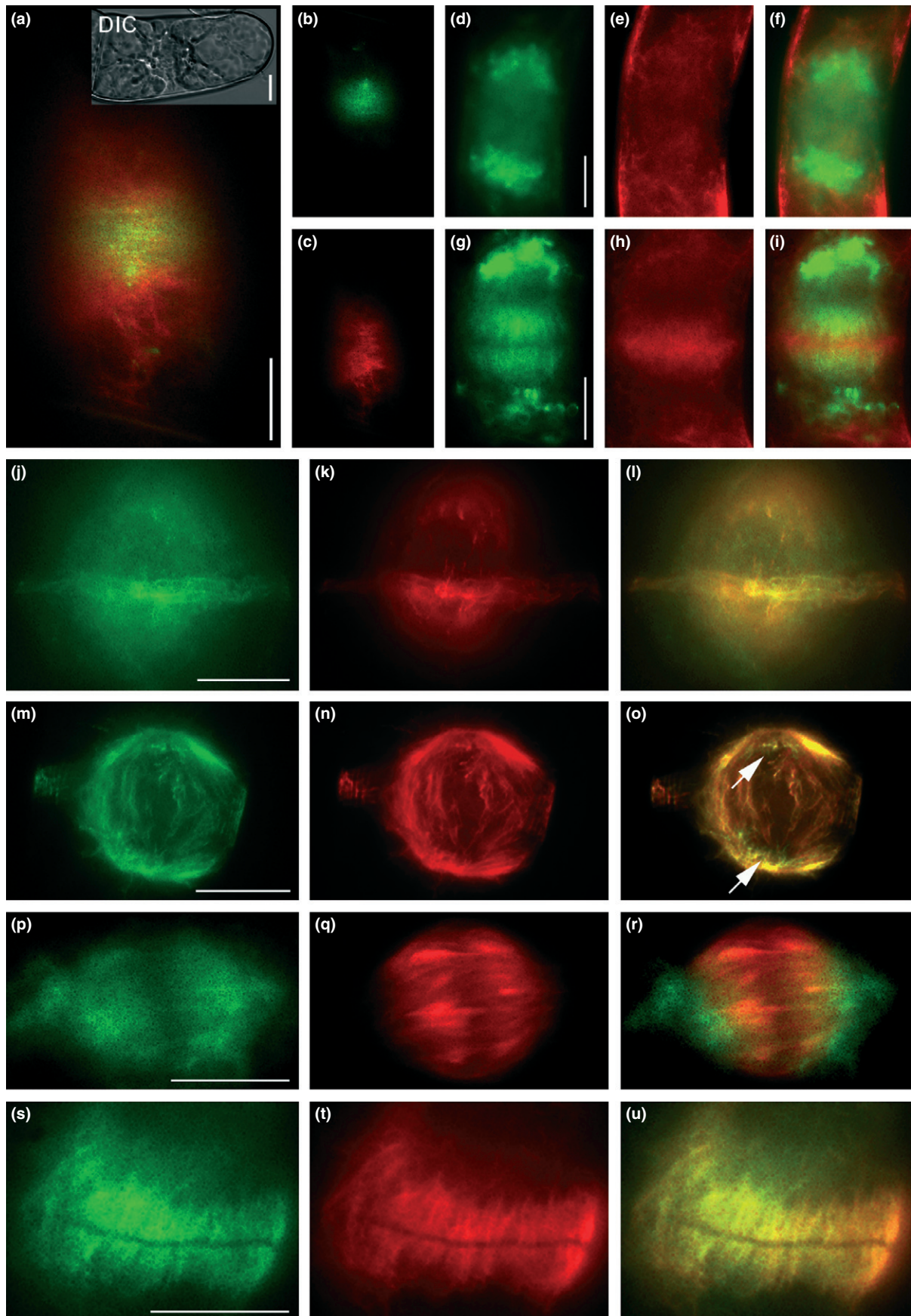
including also the closest homologue of NtKCH, the uncharacterized KCH 'AtO22260' (Menges *et al.*, 2003, 2005), suggesting a similar plant-specific function during mitosis. NtKCH transcripts were abundant in pro-metaphase, indicating a possible role during the early steps of mitosis. However, as condensed chromosomes are not transcriptionally active, mRNAs, which are needed during or immediately after metaphase, must be transcribed already at the G2/M transition. Moreover, during the course of synchronization, NtKCH transcripts declined at a slower rate than the MI, as expected for a putative function in mitosis.

Our localization studies demonstrate that intracellular KCH is dynamically redistributed during mitosis. During G2 phase, the expression of static NtKCH on the nuclear surface increased and became progressively restricted to the prospective spindle poles, where it persisted throughout metaphase (Fig. 6a–c), whereas cortical KCH vanished with the breakdown of the PPB (Fig. 6b,c). NtKCH remained excluded from the midzone (Fig. 6c) and did not align with microtubules of the metaphase spindle. This recalls the pattern of the *A. thaliana* homologue AtKinG on expression in BY-2 (Buschmann *et al.*, 2011). Overexpressed fluorescent fusions of AtKinG disappeared from the site of chromosome segregation, except in a small number of cells, where it associated with spindle microtubules leading to abnormal spindles, possibly resulting from bundling of microtubule minus-ends. As spindles of BY-2 cells stably overexpressing either OsKCH1 (Frey *et al.*, 2010) or NtKCH (this work) were completely normal, KCH apparently does not participate in the organization of the spindle itself. The localization pattern of GFP-NtKCH during metaphase rather supports a function at the spindle poles.

In telophase, bright GFP-NtKCH speckles accumulated asymmetrically at the side of the nuclei facing the prospective cell plate. Moreover, dynamic NtKCH reappeared in the midzone and strongly accumulated at the phragmoplast (Fig. 6d). As the NtKCH signal moved towards the minus-ends of phragmoplast microtubules, a participation in vesicular transport towards the cell plate is not very likely. By contrast, the direction of movement rather indicates a function of NtKCH in phragmoplast expansion or the organization of phragmoplast poles by bundling microtubular minus-ends, as proposed for KCBP (Bowser & Reddy, 1997). Unlike the cotton GhKCH2 (Xu *et al.*, 2009), we did not observe NtKCH in the centre of phragmoplasts, arguing against cross-linking with the actin filaments in the phragmoplast centre. With the formation of the new cell wall, we observed an increase in fluorescence around the daughter nuclei, with a concomitant disappearance of GFP-NtKCH signals at the decomposing phragmoplast (Fig. S2). Furthermore, distinct punctate fluorescent signals moved along phragmoplast microtubules to the nuclear surface, where they accumulated symmetrically as bright fluorescent speckles (Fig. 6e; Fig. S3). This could be a result of a recruitment of new dynamic KCH from the phragmoplast microtubules into the perinuclear region.

Functional switch and sliding model

In plant cells that prepare for division, typically, migration of the nucleus occurs towards the site at which the prospective cell plate will form (Nick, 2008). This nuclear migration is highly sensitive to inhibitors of microtubules and microfilaments (Katsuta & Shibaoka, 1988; Katsuta *et al.*, 1990), indicating a tight interplay
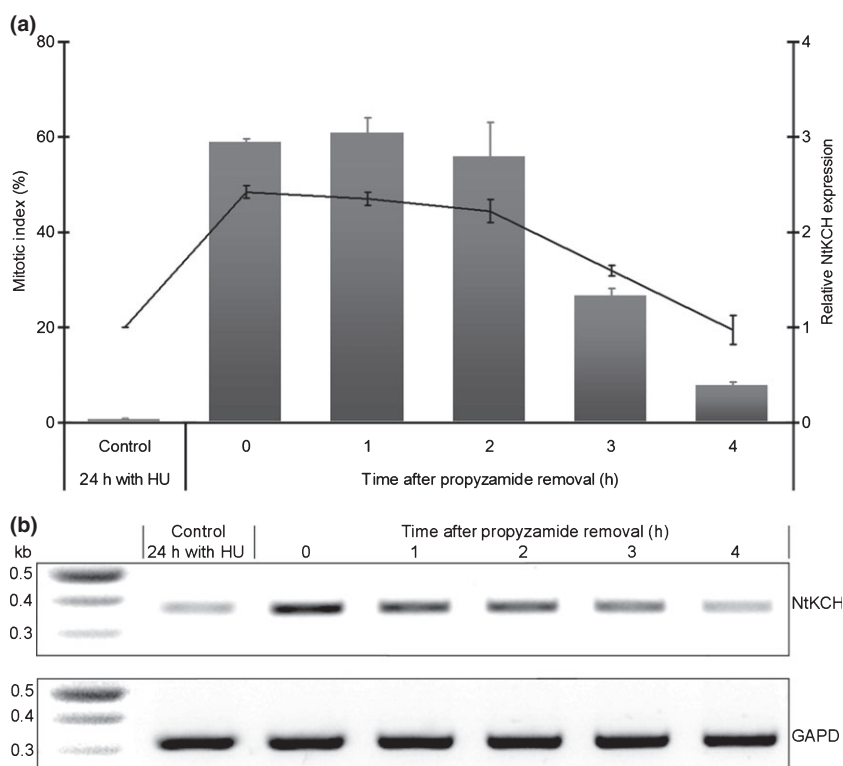
Fig. 5 NtKCH mRNA expression at different phases of the cell cycle in synchronized tobacco (*Nicotiana tabacum*) BY-2 cells. (a) Relative NtKCH expression (black curve, right *y*-axis) and the mitotic index (MI) (grey bars, left *y*-axis) after treatment with hydroxyurea (HU) for 24 h, and at 0 h and intervals of 1 h after release from propyzamide treatment. The cells were collected at the indicated time points, MI was measured and NtKCH transcription was determined by semi-quantitative reverse transcription-polymerase chain reaction (RT-PCR) using glyceraldehyde-3-phosphate dehydrogenase (GAPD) as internal standard. Mean values ± SE for each sample were estimated from at least three independent experiments. (b) Representative RT-PCR detection of NtKCH expression in synchronized BY-2 cells. The bottom lane represents the GAPD expression that was used as loading control.
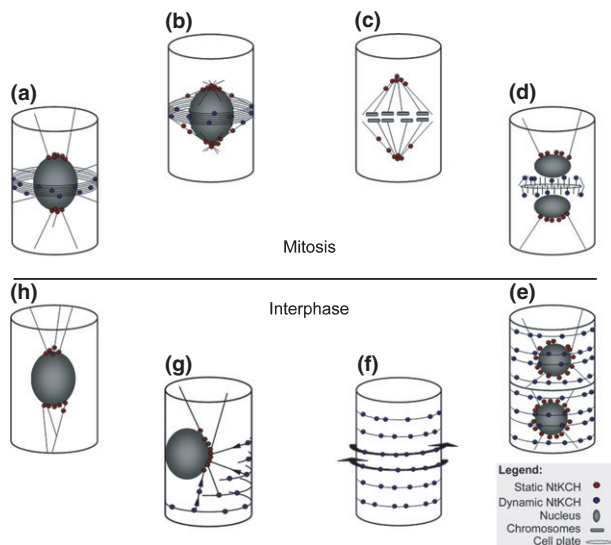
Fig. 6 Model of cell cycle-dependent NtKCH redistribution in tobacco (*Nicotiana tabacum*) BY-2 cells. The working model suggests the existence of two different NtKCH populations. During interphase, dynamic NtKCH (blue dots in e–g) exert minus-end-directed movement along transverse cortical microtubules (cMTs), whereas static residues (red dots) are restricted to the cytoskeleton of the nuclear envelope (g, h). (g) Radial microtubules are used as tracks, guiding dynamic KCHs from the cMTs to the nuclear envelope, where they are trapped as static residues by a molecular capture mechanism. (a, b, h) At late G2, static NtKCH accumulates at the prospective spindle poles. At this step, dynamic NtKCH disappears from the cortex following the breakdown of the pre-prophase band (PPB) and nuclear envelope. (c) During metaphase, exclusively static NtKCH can be found at the spindle poles. (d) In telophase, dynamic kinesins re-emerge and move towards the minus-ends of phragmoplast microtubules. When the daughter cells have separated, dynamic KCHs again localize to the cortical array of microtubules, whereas static KCHs redistribute in the perinuclear region.

between both types of element. KCHs, accumulating on the nuclear surface and cross-linking microtubules with actin filaments, are most probably involved in nuclear migration before cell division. Indeed, overexpression of OsKCH1 in BY-2 cells delayed nuclear migration and thus the onset of the first mitotic division (Frey *et al.*, 2010). Two different scenarios for the role of KCHs for nuclear movement have been proposed, relying on a 'sliding' vs a 'pulling/pushing' mechanism (Frey *et al.*, 2010). In a 'pulling/pushing' model, radial microtubules bridging the nuclear surface to the cortical layer are anchored at both sides by static KCH (or protein complexes including KCHs), and nuclear movement results from growth and shrinkage of the microtubules themselves. However, in the 'sliding' model, microtubule minus-ends are fixed in the perinuclear network by static KCHs, whereas the plus-ends are captured by KCH motors anchored in the cortex, but move towards microtubule minus-ends, generating sliding forces that act on the nucleus. Thus, a sliding mechanism implies two KCH subpopulations, which is consistent with our present findings. However, we cannot exclude the possibility that other kinesins might also contribute to this mechanism. Based on our present localization studies and the biochemical properties of KCHs (Xu *et al.*, 2007; Frey *et al.*, 2009; Umezu *et al.*, 2011), we propose that KCHs alternate between a dynamic and a static

state, and that conversion is mediated by a cell cycle-dependent capture mechanism. In this model, radial microtubules are used as tracks, guiding dynamic KCHs from the cMTs to the nuclear envelope (Fig. 6g, arrows). Such an inward movement was often observed, especially towards the onset of mitosis (Fig. 3f–i; Movie S2). On their way towards the cell centre, the dynamic properties of the kinesins would be altered by an unknown regulating factor. Biochemical analysis of recombinant expressed OsKCH1 fragments revealed that actin significantly reduces the microtubule-dependent ATPase activity of the kinesin motor by interaction with the N-terminal CH domain (Umezu *et al.*, 2011). Therefore, the actin of the dense perinuclear network itself could serve as a regulating factor changing the dynamic behaviour of KCHs. Reduced processivity would consequently lead to an accumulation of the kinesin around the nucleus, which could, in turn, result in the formation of dimers or oligomers. Oligomerization is the most straightforward explanation for the brightly fluorescent speckles, as it is a common structural feature of kinesins (Miki *et al.*, 2005). OsKCH1 from rice was found to assemble into dimers and tetramers by size exclusion chromatography and split-yellow fluorescent protein (YFP) assays (Frey *et al.*, 2010). As predicted by our *in silico* analysis, NtKCH also harbours putative coiled-coil regions upstream and at the very end of the motor core. Proteins with two CH domains in tandem cross-link F-actin, bundle actin or, in animal cells, crosswire intermediate filaments (Richardson *et al.*, 2006). A single CH domain, however, is not sufficient for actin binding (Gimona *et al.*, 2002; Korenbaum & Rivero, 2002). As KCHs only contain one CH domain in their N-terminal part, dimerization or oligomerization, generating complexes with multiple CH domains, would allow for actin binding, and thus for the appropriate positioning of the nucleus at the onset of mitosis.

Conclusions

We have isolated a new KCH from tobacco and followed its regulation and distribution throughout the cell cycle; we conclude that KCHs function in both cell elongation and cell division. To dissect these functions in their biological context, we are presently analysing specific phenotypes in rice mutants, where KCHs have been inactivated by insertion of the *Tos17* retrotransposon. Based on the present findings, we identified two populations of KCHs, which differed in their subcellular localization, dynamics and potential ability to cross-link microtubules and actin filaments. Thus, KCHs are able to change their dynamic properties, leading to a model of a cell cycle capture mechanism serving as a molecular switch. However, our knowledge of the molecular details remains incomplete. The observed changes in KCH dynamics suggest a regulation of motor activity, most probably by actin itself and/or other unknown factors. Furthermore, the preferential binding of KCHs to microtubules and/or actin (or even only a subset of actin filaments) seems to be under cell cycle-dependent control. In order to understand the differential interaction with both types of cytoskeletal filament in more detail, it will be necessary to investigate the KCH distribution and repartition with respect to the different cell cycle-dependent microtubule structures in living

cells. We have therefore already made some first attempts to generate double-transformed BY-2 cells co-expressing a fluorescent NtKCH fusion together with a microtubule marker, which will also allow us to confirm the present data from immunolocalization. However, the elucidation of the signals and factors participating in the regulation of KCH affinity to either actin or microtubules will be the most challenging task for the future in order to determine the cellular function of this group of motor proteins unique to the plant kingdom.

Acknowledgements

References

Ambrose JC, Li W, Marcus A, Ma H, Cyr R. 2005. A minus-end directed kinesin with plus-end tracking protein activity is involved in spindle morphogenesis. *Molecular Biology of the Cell* **16**: 1584–1592.

Bowser J, Reddy ASN. 1997. Localization of a kinesin-like calmodulin-binding protein in dividing cells of *Arabidopsis* and tobacco. *The Plant Journal* **12**: 1429–1437.

Breitling F, Little M. 1986. Carboxy-terminal regions on the surface of tubulin and microtubules. Epitope locations of YOL1/34, DM1A and DM1B. *Journal of Molecular Biology* **189**: 367–370.

Buschmann H, Green P, Sambade A, Doonan JH, Lloyd CW. 2011. Cytoskeletal dynamics in interphase, mitosis and cytokinesis analysed through *Agrobacterium*-mediated transient transformation of tobacco BY-2 cells. *New Phytologist* **190**: 258–267.

Cai G, Cresti M. 2010. Microtubule motors and pollen tube growth – still an open question. *Protoplasma* **247**: 131–143.

Campbell RE, Tour O, Palmer AE, Steinbach PA, Baird GS, Zacharias DA, Tsien RY. 2002. A monomeric red fluorescent protein. *Proceedings of the National Academy of Science, USA* **99**: 7877–7882.

Chandra R, Salmon ED, Erickson HP, Lockhart A, Endow SA. 1993. Structural and functional domains of the *Drosophila* ncd microtubule motor protein. *The Journal of Biological Chemistry* **268**: 9005–9013.

Collings DA. 2008. Crossed-wires: interactions and cross-talk between the microtubule and microfilament networks in plants. In: Nick P, ed. *Plant microtubules*. Berlin, Heidelberg: Springer Verlag, 47–79.

Deeks MJ, Fendrych M, Smertenko A, Bell KS, Oparka K, Cvrckova F, Zarsky V, Hussey PJ. 2010. The plant formin AtFH4 interacts with both actin and microtubules, and contains a newly identified microtubule-binding domain. *Journal of Cell Science* **123**: 1209–1215.

Endow SA. 1999. Determinants of molecular motor directionality. *Nature Cell Biology* **1**: 163–167.

Endow SA, Kang SJ, Satterwhite LL, Rose MD, Skeen VP, Salmon ED. 1994. Yeast Kar3 is a minus-end microtubule motor protein that destabilizes microtubules preferentially at the minus ends. *EMBO Journal* **13**: 2708–2713.

Euteneuer U, Jackson WT, McIntosh JR. 1982. Polarity of spindle microtubules in *Haemanthus* endosperm. *Journal of Cell Biology* **94**: 644–653.

Frey N. 2010. *Dynamic bridges: an unconventional rice kinesin links actin and microtubules*. PhD thesis, Karlsruhe Institute for Technology (KIT), Karlsruhe, BW, Germany.

Frey N, Klotz J, Nick P. 2009. Dynamic bridges: a calponin-domain kinesin from rice links actin filaments and microtubules in both cycling and non-cycling cells. *Plant and Cell Physiology* **50**: 1493–1506.

Frey N, Klotz J, Nick P. 2010. A kinesin with calponin-homology domain is involved in premitotic nuclear migration. *Journal of Experimental Botany* **61**: 3423–3437.

Gimona M, Djinovic-Carugo K, Kranewitter WJ, Winder SJ. 2002. Functional plasticity of CH domains. *FEBS Letters* **513**: 98–106.

Goode BL, Drubin DG, Barnes G. 2000. Functional cooperation between the microtubule and actin cytoskeletons. *Current Opinion in Cell Biology* **12**: 63–71.

Guindon S, Dufayard JF, Lefort V, Anisimova M, Hordijk W, Gascuel O. 2010. New algorithms and methods to estimate maximum-likelihood phylogenies: assessing the performance of PhyML3.0. *Systematic Biology* **59**: 307–321.

Guindon S, Gascuel O. 2003. A simple, fast, and accurate algorithm to estimate large phylogenies by maximum likelihood. *Systematic Biology* **52**: 696–704.

Hancock WO, Howard J. 1998. Processivity of the motor protein kinesin requires two heads. *Journal of Cell Biology* **140**: 1395–1405.

Hartley JL, Temple GF, Brasch MA. 2000. DNA cloning using *in vitro* site-specific recombination. *Genome Research* **10**: 1788–1795.

Hu TX, Yu M, Zhao J. 2010. Comparative transcriptional profiling analysis of the two daughter cells from tobacco zygote reveals the transcriptome differences in the apical and basal cells. *BioMed Central Plant Biology* **10**: 167.

Karimi M, Inzé D, Depicker A. 2002. Gateway vectors for *Agrobacterium*-mediated plant transformation. *Trends in Plant Science* **7**: 193–195.

Katsuta J, Hashiguchi Y, Shibaoka H. 1990. The role of the cytoskeleton in positioning of the nucleus in premitotic tobacco BY-2 cells. *Journal of Cell Science* **95**: 413–422.

Katsuta J, Shibaoka H. 1988. The roles of the cytoskeleton and the cell wall in nuclear positioning in tobacco BY-2 cells. *Plant and Cell Physiology* **29**: 403–413.

Korenbaum E, Rivero F. 2002. Calponin homology domains at a glance. *Journal of Cell Science* **115**: 3543–3545.

Kumagai F, Hasezawa S. 2001. Dynamic organization of microtubules and microfilaments during cell cycle progression in higher plant cells. *Plant Biology* **3**: 4–16.

Letunic I, Bork P. 2007. Interactive Tree Of Life (iTOL): an online tool for phylogenetic tree display and annotation. *Bioinformatics* **23**: 127–128.

Lupas A, Van Dyke M, Stock J. 1991. Predicting coiled-coils from protein sequences. *Science* **252**: 1162–1164.

Maisch J, Fiserova J, Fischer L, Nick P. 2009. Tobacco Arp3 is localized to actin-nucleating sites *in vivo*. *Journal of Experimental Botany* **60**: 603–614.

Marcus AI, Ambrose JC, Blickley L, Hancock WO, Cyr RJ. 2002. *Arabidopsis thaliana* protein, ATK1, is a minus-end directed kinesin that exhibits non-processive movement. *Cytoskeleton* **52**: 144–150.

Matsui K, Collings D, Asada T. 2001. Identification of a novel plant-specific kinesin-like protein that is highly expressed in interphase tobacco BY-2 cells. *Protoplasma* **215**: 105–115.

Menges M, de Jager SM, Gruissem W, Murray JA. 2005. Global analysis of the core cell cycle regulators of *Arabidopsis* identifies novel genes, reveals multiple and highly specific profiles of expression and provides a coherent model for plant cell cycle control. *Plant Journal* **41**: 546–566.

Menges M, Hennig L, Gruissem W, Murray JA. 2003. Genome-wide gene expression in an *Arabidopsis* cell suspension. *Plant Molecular Biology* **53**: 423–442.

Miki H, Okada Y, Hirokawa N. 2005. Analysis of the kinesin superfamily: insights into structure and function. *Trends in Cell Biology* **15**: 467–476.

Mineyuki Y. 1999. The preprophase band of microtubules: its function as a cytokinetic apparatus in higher plants. *International Review of Cytology* **187**: 1–49.

Nagata T, Nemoto Y, Hasezawa S. 1992. Tobacco BY-2 cell line as the "HeLa" cell in the cell biology of higher plants. *International Review of Cytology* **132**: 1–30.

Nick P. 2008. Control of cell axis. In: Nick P, ed. *Plant microtubules*. Berlin, Heidelberg: Springer Verlag, 23–46.

Panteris E. 2008. Cortical actin filaments at the division site of mitotic plant cells: a reconsideration of the 'actin-depleted zone'. *New Phytologist* **179**: 334–341.

Paredez AR, Somerville CR, Ehrhardt DW. 2006. Visualization of cellulose synthase demonstrates functional association with microtubules. *Science* 312: 1491–1495.

Petrásek J, Schwarzerová K. 2009. Actin and microtubule cytoskeleton interactions. *Current Opinion in Plant Biology* 12: 728–734.

Preuss ML, Kovar DR, Lee YR, Staiger CJ, Delmer DP, Liu B. 2004. A plant-specific kinesin binds to actin microfilaments and interacts with cortical microtubules in cotton fibers. *Plant Physiology* 136: 3945–3955.

Reddy AS. 2001. Molecular motors and their functions in plants. *International Review of Cytology & Cell Biology* 204: 97–178.

Reddy AS, Day IS. 2001. Kinesins in the *Arabidopsis* genome: a comparative analysis among eukaryotes. *BioMed Central Genomics* 2: 2.

Richardson DN, Simmons MP, Reddy AS. 2006. Comprehensive comparative analysis of kinesins in photosynthetic eukaryotes. *BioMed Central Genomics* 7: 18.

Rodriguez OC, Schaefer AW, Mandato CA, Forscher P, Bement WM, Waterman-Storer CM. 2003. Conserved microtubule–actin interactions in cell movement and morphogenesis. *Nature Cell Biology* 5: 599–609.

Sakai T, Honing H, Nishioka M, Uehara Y, Takahashi M, Fujisawa N, Saji K, Seki M, Shinozaki K, Jones MA et al. 2008. Armadillo repeat-containing kinesins and a NIMA-related kinase are required for epidermal-cell morphogenesis in *Arabidopsis*. *The Plant Journal* 53: 157–171.

Samuels AL, Meehl J, Lipe M, Staehelin LA. 1998. Optimizing conditions for tobacco BY-2 cell cycle synchronization. *Protoplasma* 202: 232–236.

Sano T, Higaki T, Oda Y, Hayashi T, Hasezawa S. 2005. Appearance of actin microfilament "twin peaks" in mitosis and their function in cell plate formation, as visualized in tobacco BY-2 cells expressing GFP-fimbrin. *Plant Journal* 44: 595–605.

Song H, Golovkin M, Reddy AS, Endow SA. 1997. *In vitro* motility of AtKCBP, a calmodulin-binding kinesin protein of *Arabidopsis*. *Proceedings of the National Academy of Science, USA* 94: 322–327.

Tamura K, Nakatani K, Mitsui H, Ohashi Y, Takahashi H. 1999. Characterization of KatD, a kinesin-like protein gene specifically expressed in floral tissues of *Arabidopsis thaliana*. *Gene* 230: 23–32.

Traas JA, Doonan JH, Rawlins DJ, Shaw PJ, Watts J, Lloyd CW. 1987. An actin network is present in the cytoplasm throughout the cell cycle of carrot cells and associates with the dividing nucleus. *Journal of Cell Biology* 105: 387–395.

Umezu N, Umeki N, Mitsui T, Kondo K, Maruta S. 2011. Characterization of a novel rice kinesin O12 with a calponin homology domain. *The Journal of Biochemistry* 149: 91–101.

Wasteneys GO, Galway ME. 2003. Remodeling the cytoskeleton for growth and form: an overview with some new views. *Annual Review of Plant Biology* 54: 691–722.

Xu T, Qu Z, Yang X, Qin X, Xiong J, Wang Y, Ren D, Liu G. 2009. A cotton kinesin GhKCH2 interacts with both microtubules and microfilaments. *Biochemical Journal* 421: 171–180.

Xu T, Sun X, Jiang S, Ren D, Liu G. 2007. Cotton GhKCH2, a plant-specific kinesin, is low-affinitive and nucleotide-independent as binding to microtubule. *Journal of Biochemistry and Molecular Biology* 40: 723–730.

Yang JT, Laymon RA, Goldstein LS. 1989. A three-domain structure of kinesin heavy chain revealed by DNA sequence and microtubule binding analyses. *Cell* 56: 879–889.

Yasuda H, Kanda K, Koiwa H, Suenaga K, Kidou S, Ejiri S. 2005. Localization of actin filaments on mitotic apparatus in tobacco BY-2 cells. *Planta* 222: 118–129.

Supporting Information

Additional supporting information may be found in the online version of this article.

Fig. S1 Treatment of GFP-NtKCH/RFP-FABD2-expressing tobacco BY-2 cells with cytoskeleton drugs.

Fig. S2 GFP-NtKCH localizes to the phragmoplast of BY-2 cells.

Fig. S3 Time-lapse series of stable GFP-NtKCH/RFP-FABD2 co-expression in BY-2 cells during cytokinesis.

Movie S1 GFP-NtKCH exhibits dynamic movement on cortical microtubules (cMTs).

Movie S2 Inward directed movement of GFP-NtKCH along radial filaments.

Movie S3 Directionality of NtKCH along phragmoplast microtubules observed in GFP-NtKCH cells.

Movie S4 Stable expression of GFP-NtKCH and RFP-FABD2 in a BY-2 cell from metaphase until the end of cytokinesis.

Please note: Wiley-Blackwell are not responsible for the content or functionality of any supporting information supplied by the authors. Any queries (other than missing material) should be directed to the *New Phytologist* Central Office.